Tide and wave driven flow across the rim reef of the atoll of Raroia (Tuamotu, French Polynesia)

Jerome Aucan, Terence Desclaux, Romain Le Gendre, Vetea Liao, Serge Andréfouët

Version of Record: https://www.sciencedirect.com/science/article/pii/S0025326X21007529
Manuscript_a60dcf872ed9d31dfff63701cebae928

Tide and wave driven flow across the atoll rim reef of the atoll of Raroia (Tuamotu, French Polynesia)

Jerome Aucan[a,*], Terence Desclaux[a], Romain Le Gendre[b], Liao Vetea[c], Serge Andréfouët[a]

[a] *Institut de Recherche Pour le Développement (IRD). UMR 9220 ENTROPIE (Institut de Recherche Pour le Développement, Université de la Réunion, IFREMER, Université de la Nouvelle-Calédonie, Centre National de la Recherche Scientifique), Nouméa, New Caledonia*
[b] *Institut Français de Recherche pour l'Exploitation de la MER, UMR 9220 ENTROPIE (Institut de Recherche Pour le Développement, Université de la Réunion, IFREMER, Université de la Nouvelle-Calédonie, Centre National de la Recherche Scientifique), Nouméa, New Caledonia*
[c] *Marine Resources Division, Government of French Polynesia*

Abstract

The currents flowing across the rim of the atoll of Raroia were investigated with a 1 year-long dataset of wave, water level and currents. Offshore waves break on the edge of the reef outside the atoll's rim and drive current into the lagoon, through the shallow *hoa* that cut across the rim. The additional water volume generated by this wave driven flow induces an elevation of water level throughout the atoll's lagoon and is evacuated back into the open ocean through a deep reef pass. The water level inside the atoll is also driven by astronomical tides, which enter the lagoon thought the reef pass, after undergoing a $\sim 50\%$ decrease in amplitude and a ~ 4 hours lag. Using a simple parametric model with three calibrated coefficients, we show that currents across the atoll's rim can be estimated as a function of the offshore wave conditions and the water level difference between the ocean and the lagoon.

Keywords: pearl farming; lagoon; coral reef; hydrodynamic

1. Introduction

The production of black pearls in the Central Pacific Ocean mostly takes place in deep ($> 25m$) atoll lagoons. The hydrology and hydrodynamics of these lagoons is an important factor for the successful farming of the black lip pearl oyster *Pinctada margaritifera*, which produces the prized pearls after the grafting in the oyster pearl sac of an artificial nucleus paired with a piece of mantle from a donor. Beyond proper handling by farmers, oysters growth

*Corresponding author
Email address: jerome.aucan@ird.fr (Jerome Aucan)

and survival at larval, juvenile and adult stages depend on adequate hydrologic conditions, in particular trophic planktonic conditions and lagoon temperature ranges (Sangare et al., 2020). These conditions are largely controlled by the exchange of water between the ocean and the lagoon, through the atoll rim and passes (Lowe and Falter, 2015).

Atoll lagoons are isolated from the nearby ocean by an atoll rim, which is typically a kilometer wide, and can have emerged, intertidal and submerged sections. In Tuamotu Archipelago (French Polynesia) the rim is typically composed of shallow reef flat channels (*hoa*) that occur between sandy cays (*motu*). The numbers of *hoa*, and their width can vary widely from one atoll to another (Andréfouët et al., 2001a). The rim can also be cut by one or more deep passes. In addition to the intrinsic rim structure, and its degree of openness to the ocean, sea level, waves, tides and wind can have a strong influence on the lagoon renewal and its physical and chemical properties, and its water circulation (Tartinville and Rancher, 2000; Andréfouët et al., 2006; Dumas et al., 2012; Charpy et al., 2012, among many others).

Wave driven flows over reefs have mostly been studied over "closed reefs" or "fringing reef" on one hand, or on "open reefs" or "barrier reef" on the other hand (Lindhart et al., 2021, as a recent example). A "closed reef" describes a reef where the leeward water level is close to or as high as the water setup on the reef (Lowe et al., 2009, for an example). An "open reef" describes a reef where water level leeward of the reef return to a water level similar to the open ocean (Monismith et al., 2013, for an example). Here we describe measurements over an "atoll rim reef" where water level leeward of the reef (in the atoll lagoon) is neither equal to the setup on the reef nor equal to the open ocean water level. Instead, water level leeward of an "atoll rim reef" is a combination of tidal elevation driven by ebb and constrained within reef passes that can be 10s of km away, and wave driven flow occuring at many other places of the atoll rim.

For the Tuamotu Archipelago atolls, where significant pearl farming takes place, there has been limited work on the water fluxes through the *hoa*, and in particular how it is related with waves in the ocean (generated by distant swells and local winds), tides and sea level. To the best of our knowledge, Lenhardt (1991); Tartinville and Rancher (2000); Dufour et al. (2001); Dumas et al. (2012) have investigated this aspect, which is critical in order to achieve the 3D numerical model of an atoll lagoon (Andréfouët et al., 2006). Specifically, Lenhardt (1991) monitored current speed in one *hoa* of Tikehau atoll. Tartinville and Rancher (2000) in Mururoa atoll, and Pagès and Andréfouët (2001) and Andréfouët et al. (2001b) in several different atolls, could compare empirically at day-scale the flows across several *hoa* with significant wave height estimated by satellite altimetry. Andréfouët et al. (2001a) in particular concluded that a linear relationship between flows and wave height could be found, although the exact relationship differed between different types of atoll rims, and possibly between atolls. Dumas et al. (2012) when developing a numerical model of lagoon circulation for Ahe atoll confirmed the effect of local conditions, as they could simply apply a constant flow in Ahe numerous, but narrow

hoa, considering how little this atoll was affected by waves most of the time, due to its geographic position protected from the incoming distant swells by nearby atolls (Andréfouët et al., 2012). However, these results generally used short series of observations, except for Ahe, and they did not really disqualify the possibility to infer a generic, rim-independent, relationship if long time series could be acquired for an atoll, or several atolls, presenting various type of rims exposed to distant swells and to local wind-generated waves as well. Such parameterization would be critical to continue developing lagoon hydrodynamic models for a variety of atolls (Le Gendre et al. in prep.).

Raroia is a $40km$ long and $12km$ wide atoll of the Central Tuamotu, with only one deep reef pass on its western side (Figure 1), numerous *hoa* on all sides of the atoll's diverse rim, and is believed to be flushed by both tide and waves from different directions. Raroia is also an important pearl oyster farming site, for both spat collecting and pearl production, although, like in many atolls, several farms have recently closed due to the crisis of the pearl farming industry. Raroia was therefore an ideal study site to develop a generic, multi-rim, model of currents through the *hoa* based on wave and tide characteristics. This simple relationship between wave height, water level and inbound current across the rim, will allow the integration of this forcing into future lagoon 3D numerical circulation models.

2. Material and methods

2.1. Study site

Raroia is a large ($368km^2$), deep (maximum depth = $68m$) atoll of the Central Tuamotu. Its lagoon geomorphology is described in detail in Andréfouët et al. (2020) from multibeam data set also acquired in preparation for the modeling of the lagoon circulation. It is oriented along NE-SW direction, offering a long stretch of rim directly exposed to the east tradewinds. This area corresponds best to the rim Type 7 described in Andréfouët et al. (2001a). This rim is characterized by small elongated or circular motu bordered by wide areas of intertidal sand, and wide shallow *hoa*. Conversely the south side of the atoll does not present any motu and corresponds to the rim type 4 (Andréfouët et al., 2001a). The western side can be related to the rim type 5 with narrow well defined sharply bounded *hoa* between wide motu that form on top of elevated ($\sim$ $1m$) conglomerate. Hence, not all rim types are present in Raroia, but there is a good variety of the semi-open (rim 5, 7) and the very open one is present (rim 4).

2.2. Site description and instrumentation

In-situ data collection lasted for almost a year over three different legs (May-Aug 2018, Aug-Dec 2018 and Jan-March 2019). We concentrated our efforts around 3 *hoa* on the western (1, rim type 7), eastern (2, rim type 5) and southern (3, rim type 4) facing sides of the atoll. Outside of each *hoa* (O1, O2, and O3), a pressure sensor was deployed on the forereef at $\sim 10m$ depth to measure offshore

waves and water level outside the atoll. Within each *hoa*, an acoustic current meter was deployed in $1-3m$ depth to measure currents and water levels (H1, H2, and H3). This sampling strategy is illustrated on Figure 1 (middle). H1 was deployed during leg 1, H3 was deployed during legs 2 and 3, and H2 was deployed on all 3 legs. Within the lagoon several pressure sensors were deployed on pinnacles at $\sim 8m$ depth to measure water level inside the atoll (L4,L5,L6,L7 and L8). Instruments positions are shown on Figure 1 (top) and characteristics are summarized in Table 1.

Water level

At the ocean sites (O), *hoa* sites (H), and lagoon sites (L), pressure sensors sampled the in-situ water pressure continuously (no burst sampling), at $1Hz$ (see Table 1). The continuous $1Hz$ pressure record was divided into 1-hour-long bursts to calculate the mean hourly water level h_{ocean} or h_{lagoon}. Between each leg, each instrument was recovered, data was offloaded, batteries were changed and the instrument was deployed again. While water level from the uncorrected pressure record on all sites showed similar short term variability, they also showed trends relative to each others that coud not have a physical explanation other than expected intrumental drift, that remained within the manufacturer's specification of 1cm/year. We therefore corrected the raw pressure data for 1) individual pressure offsets due to a change in vertical position between leg or an instrumental bias, and 2) linear drift of individual instruments. The measured trend at each instrument during each leg is the combination of the instrument drift and the actual water level trend. We calculated an average trend across all sites for each leg, which we considered as the actual water level trend (assuming individual drifts would cancel each others). To correct each instrumental pressure records, for each leg, we therefore removed the individual trends at each instrument before adding back the common trend. The resulting corrected time-series are shown on (Figure 2).

Daily values of water level were subsequently obtained from the hourly water level values by applying a Demerliac filter (Bessero, 1985) to remove the effects of the astronomical tide and resampled to daily time-steps. Tidal phases and amplitudes were calculated using the Matlab Utide package (Codiga, 2011).

Wave characteristics

Each burst was subjected to a Fourier analysis to obtain pressure spectra $S_p(f)$ at frequency f in the $3-25s$ period band. The pressure spectra $S_p(f)$ was converted into sea-surface elevation spectra $S(f)$ using linear wave theory after removal of a constant atmospheric pressure value of 1013 hPa. We then calculated significant wave height H_{sig} as $4\times\sqrt{\sum S(f)df}$ and the mean period T_{m01} as $\frac{\sum f^{-1}S(f)}{\sum S(f)}$. Since we are interested in reef processes, we also calculated a breaking wave height equivalent $H_b = H_{sig}^{4/5}T_{m01}^{2/5}$ using a parameterization similar to that of Caldwell and Aucan (2007) , Hench et al. (2008) or Merrifield et al. (2014), with a shore-normal propagation angle.

Currents

At the *hoa* sites (H) (see Table 1), current profilers measured current speed and direction in 12 vertical bins each $20cm$ high. The valid bins were selected based on the measured water depth above the instrument. We used a depth average over the valid vertical bins to calculate the mean current vector $\vec{U} = [u_1, v_1]$. We then calculated the principal direction θ of the current by solving in the least square sense $v_1 = a \times u_1 + b$ with $\theta = atan(a)$ (i.e., the yellow lines on Figure 5). The principal current direction should be predominantly along the axis of the *hoa*, perpendicular to the atoll rim (Figure 1 and Figure 5). For the rest of the paper, we only consider the current speed along the principal direction θ, where U refers to the current projected on this principal direction. Daily values of current speed were obtained from the hourly values by applying a Demerliac filter (Bessero, 1985) and a daily resampling, to remove the effects of the astronomical tide.

Parametric model

The aim of this study is to relate the current speed in the *hoa* to the wave and water level condition in a parametric, and generic sense, and for further inclusion into a lagoon circulation model (ie Le Gendre et al. in prep.). To guide us, there has been numerous previous studies on how to relate waves to across-reef flow (Symonds et al., 1995; Hearn, 1999; Gourlay and Colleter, 2005; Bonneton et al., 2007; Hench et al., 2008; Chevalier et al., 2015), although not specific to atoll rim environments. One of the key forcing parameters of across-reef flow is offshore wave conditions (wave height H_{sig} and wave period T_{m01}) or the breaking wave height (H_b), which drive wave setup in the breaking zone and across-reef flow downstream of the breaking zone. To simulate the water speed component in the *hoa* that is only due to the waves (e.g. the daily-averaged current), we can use a simple model based on equation 1, with the daily average (e.g. de-tided) values.

$$U_{daily} = AH_b + C \tag{1}$$

where U is the current, H_b is the breaking wave height equivalent, and A and C are constants. The breaking wave height equivalent $H_b = H_{sig}^{4/5} T_{m01}^{2/5}$, obtained by conserving the wave energy flux from offshore to the break point (Caldwell and Aucan, 2007; Hench et al., 2008) for a shore normal incoming wave. For each *hoa* and each leg, these constants were optimized in the least-square sense, in order to give the best fit to measured values of U_{daily}. We note that the dimensions in our equation 1 don't reflect the dimensions of the momentum equation normally used for "closed reefs" or "open reefs" as in Lindhart et al. (2021). In this case, our equation balances the wave forcing with the friction, averaging over the tidally driven pressure gradient.

Another key forcing parameter of across-reef flow is the water level downstream of the surf zone which controls the flow of water across the reef. Symonds et al. (1995); Hearn (1999); Tartinville and Rancher (2000) make the hypothesis that water level within the lagoon, downstream of the surf zone is the same as

offshore (e.g. the outgoing flow through reef passes is unrestricted enough to compensate the incoming wave driven cross-reef flow). In Gourlay and Colleter (2005), there are no such hypothesis. In our case, the water level inside the lagoon is also tidally driven, with a phase lag of several hours compared to the open ocean (see Table 3 and section below). Hence, the water level downstream of the surf zone, across the *hoa* is controlled by the tide, and the lagoon wide return flow through the reef pass. To simulate hourly currents in the *hoa*, with a dependence on both tidal elevation changes and wave height, we included a pressure gradient term in equation 1 :

$$U_{hourly} = AH_b + B[(h_{ocean} - \overline{h_{ocean}}) - (h_{lagoon} - \overline{h_{lagoon}})] + C \qquad (2)$$

where H_b is the breaking wave height equivalent, h_{ocean} is the sea-level height outside the reef, h_{lagoon} is the sea-level height inside the lagoon, the overbar designate time-averaged quantities and A, B and C are constants. The first term represents the effect of waves, the second term represents the effect of water level difference between ocean and lagoon, and the third is a constant. For each *hoa* and each leg, these constants were optimized in the least-square sense, in order to give the best fit to measured values of U_{hourly}. Similarly to the classic momentum balance equation Lindhart et al. (2021, for a recent study) equation 2 is simply balancing a pressure gradient, a radiation stress (the wave forcing), and a friction term (the velocity term).

3. Results

Water level

Outside the atoll, hourly sea level variations are predominantly tidal ($\sim 98\%$ of the sea level variability explained by a tidal harmonic analysis), with a strong dominance of the semidiurnal components (Table 2). Daily water levels outside the atoll varied by a few cm over the course of the study (Figure 2 top), due to large scale ocean features, and are comparable to time-series of sea level anomalies products from satellite altimetry (not shown). Transient differences between water level among the ocean sites can be attributed to passing meso-scale eddies with horizontal length scales smaller than the atoll. We note that large scale currents could also cause such differences (Rogers et al., 2017).

Within the atoll, daily sea level variations were an order of magnitude higher than on the ocean side (Figure 2 bottom), and can vary by tens of cm during the course of a few days. Compared to the ocean sites, only 60 to 70% of the hourly sea level variability could be explained by a tidal harmonic analysis (Table 2). This higher variability and lesser tidal character of sea level inside the atoll compared to outside was attributed to wave events that drive water inside the atoll through the *hoa*.

We note that there was little geographical variation of daily sea level values within the atoll (Figure 2 bottom). There wasn't also any lag between tidal constituent within the atoll, indicating the sea level within the lagoon varies

uniformly at hourly and daily time scales. There was a factor ~ 2 attenuation for all semidiurnal amplitudes (Table 2) and a lag of $3-4$ hours between the ocean tide and the lagoon tide (Table 3). This can be explained by the strong flow restriction at the reef pass, which is the only unobstructed passage across the atoll rim. These observations are comparable to those of Dumas et al. (2012) in the nearby Ahe atoll in the Western Tuamotu.

3.1. Waves

Waves in Raroia atoll come from 3 main generation areas during the studied period : low frequency waves from the NW (SW) are generated remotely by mid to high latitude winter storms in the northern (southern) hemisphere, and high frequency waves from the E are generated by the local trade wind (Dutheil et al., 2020, and their Figure 5). Given the atoll rim orientation at each site, low frequency waves from the NW were prevalent at O1/H1 during November to April, where wave height could episodically reach $2m$. Low frequency SW waves were prevalent at O3/H3 from June to October with wave heights up to $3m$. Finally, high frequency trade wind seas were prevalent at O2/H2 nearly year-round with heights also up to $3m$ (Figures 3 and 4).

3.2. Currents in the hoa

Daily averaged currents in the *hoa* were always lagoon-ward and could reach 0.5 to $0.6m.s^{-1}$ (Figures 5 and 6). We will show later that the daily current is driven by waves. Hourly currents in the *hoa* exhibited a strong semidiurnal variability due to the tide (not shown).

3.3. Parametric model

The modeled daily-averaged current was in good agreement with the observations (Figure 6). For each individual leg and site, the correlation between observed and modeled current is above 0.95 except for one data set (leg 3 at H2), and the range-normalized RMSE is always below 10% (Table 4). The values of the parameters A and C vary by a factor ~ 2. If we use the mean values of A and C and try to generalize our model, the correlation remains almost the same as before, and the RMSE is increasing (Table 5), up to 32% at one site.

The modeled hourly-averaged current was in good agreement with the observations (example in Figure 7, top). For each individual leg and site, the correlation between observed and modeled current is above 0.9 except for one leg (leg 3 at H2), and the range-normalized RMSE is always below 10% (Table 6). The values of the parameters A, B and C vary by a factor ~ 2. If we use the mean values of A and B and C and try to generalize our model, the correlation remains almost the same as before, and the RMSE is increasing (Table 5), but less than for the daily model ($< 16.5\%$ at all sites and legs).

4. Discussion

The aim of this study was to provide a simple parameterization of currents in the *hoa*, so that these currents can be taken into account in a 3D circulation model of the atoll. Because this parameterization is to be included in a 3D circulation model, the model variables also need to be limited to those available from the 3D circulation model (e.g. water level inside or outside the lagoon) or through other readily available sources (offshore wave conditions from regional or global wave models such as Dutheil et al. (2020)). A high resolution 3D model resolving the driving process in play would require a high resolution digital elevation map. However, in our case, only bathymetric data in navigable areas (hence relatively deep) was available. Elevation and bathymetric data in the *hoa* and the reef crest were not available.

Furthermore, we used a very simple model because we had data only at a limited number of points (one offshore, one in the *hoa* and one in the lagoon, on each ocean-*hoa*-lagoon transect). With this limitation we could not study the processes more thoroughly (for example, we have no data in the surf zone). However, since we have data for a long period (1 year), we collected a wide range of conditions, allowing us to properly estimate the strength of our model, unlike shorter experiments.

We chose a formulation based on previous work (Gourlay and Colleter, 2005; Hench et al., 2008; Lindhart et al., 2021, etc...), but with some adaptations. The equation used balances a radiation stress gradient (the wave driven term), a pressure gradient (the water level term) and a friction term (the velocity). The wave-driven term (first term in equations 1 and 2) describes the process in which waves break, generate a wave setup which then drives a flow downstream in the lagoon through the *hoa*. It is always positive, directed toward the lagoon. It uses the formulation of the breaking wave height equivalent $H_b = H_{sig}^{4/5} T_{m01}^{2/5}$, obtained by conserving the wave energy flux from offshore to the break point (Caldwell and Aucan, 2007; Hench et al., 2008). More precisely, the exact formulation is $H_b = H_{sig}^{4/5} T_{m01}^{2/5} g^{1/5} \gamma^{1/5} (8\pi)^{-2/5} cos(\theta)^{2/5}$, where γ is the breaking point parameter, θ is the propagation angle relative to the shore-normal, and g is the gravity constant (Hench et al., 2008). Here, a shore-normal propagation is assumed at all times. It is a reasonable assumption since we measure wave height really close to shore (in $\sim 10m$ depth). In addition, we did not measure wave direction, so we could not test whether releasing this assumption would improve the model performance. For future usage, if wave conditions are obtained from further offshore, then one could use $H_b = H_{sig}^{4/5} T_{m01}^{2/5} cos(\theta)^{2/5}$. The breaking parameter γ relates the water depth to the wave height at the breaking point. In our formulation, γ is considered constant with time, and is included in the constant A, along with the other fixed terms in the theoretical H_b formulation.

The water level difference term describes the flow generated across the *hoa* by a difference in water level. We lack absolute measurements of the slope between ocean and lagoon because the bottom-mounted pressure sensors used

to measure water level in the ocean and the lagoon were too far apart (and too deep) to be related to each other. Given the tidal regime in the atoll with the phase lag between ocean and lagoon (discussed above), there are also no time when we could make the assumption that water levels inside and outside are equal (e.g when waves are small). In our formulation, we therefore used the variations of water level around their respective time-average. The flow predicted by this term can therefore be directed either way : a higher (lower) water in the lagoon can drive flow out of (into) the lagoon. The constant term B is equivalent to a friction coefficient. The constant term C in the equations 1 and 2 compensates the cases where waves are small (hence, not driving any current), yet the formulation of equations 1 and 2 still predicts a wave-driven current. Any time-averaged water level difference between ocean and lagoon would also be represented by the constant term C. The respective contribution of these 3 terms is illustrated on Figure 7, bottom.

The A, B and C parameters of the equations 1 and 2 were optimized for each site and leg, and all values are within a factor 2 of each other, whether comparing sites during the same leg, or during different leg for the same site. We tested whether we could generalize our parametrization to all *hoa* sites and leg with one set of parameters. To do so, values of the "optimized" constants A, B and C were averaged, to provide a "mean" set of parameter. The currents were simulated with these parameters in equations 1 and 2, and the quality of the simulation was estimated (see Tables 5 and 7). This robustness analysis showed good results. The performance remained very satisfactory in terms of correlation, and the RMSE remained below 33% for daily simulations, and below 16% for hourly simulations. Small transient offsets appear between timeseries of modeled and observed velocities (figures 6 and 7) that we could attribute to 1) processes not included in the model (wind) 2) wave driven processes occurring at other hoas around the atoll, or inherent limitations of our simple model. Nonetheless, a very simple parametrization was found to be able to account for the wide variety of wave and tide conditions that the *hoa* experienced, and to simulate the speed of water passing through them. More precisely: the parametrization provides very good timing of the events - as quantified by the correlation coefficient - and a good estimate of their magnitude – as quantified by the RMSE. This is a very noticeable result, as, to the best of our knowledge, it had never been reported in the Tuamotu region. This implies that we have good confidence with regard to the extension of the parametrization to other periods of time or islands with similar geomorphology.

Our observations of dominant inflows through *hoa* match reports from other atolls. Besides Ahe atoll already mentioned Dumas et al. (2012); Kench and McLean (2004) observed in an atoll of the Indian Ocean, small outflowing hourly currents in the *hoa*, but overall, the hourly currents were predominantly lagoonward (figures 5 and 7). In Manihiki, a pearl farming atoll in the Cook Islands, there is no deep pass Andréfouët et al. (2020), and the circulation across the rim is different than atolls with passages. For this atoll, and Rakahanga as well, inflows by waves fill the lagoon in the exposed part of the rim (as described for Raroia), but *hoa* on the opposite side of the rim also drive by gravity the excess

amount of water outwards during the tidal cycle (Callaghan et al., 2006). These outbound processes could also be simulated with our simple model : One the wave exposed *hoa*, the wave term $A \times H_b$ is larger than the water level term $B \times ((h_{ocean} - \overline{h_{ocean}}) - (h_{lagoon} - \overline{h_{lagoon}}))$ so the modeled flow is directed into the lagoon, and on the non-exposed *hoa*, the wave term is zero, and the water level term $B \times ((h_{ocean} - \overline{h_{ocean}}) - (h_{lagoon} - \overline{h_{lagoon}}))$ drives an outward flow.

5. Conclusion

We collected for the first time in a Tuamotu atoll environment, a nearly 1-year long dataset of oceanic wave, lagoon water level and currents across the Raroia atoll rim. The data set allowed defining a multi-rim generic and simple relationship between wave height and inbound current across the rim, in order to integrate this forcing into future lagoon 3D numerical models. We found that in Raroia Atoll, daily (hourly) currents in the *hoa* were always (predominantly) flowing into the lagoon, and are dependent on both offshore wave conditions and water level difference between ocean and lagoon.

Water level inside the atoll was driven 60 to 70% by the tide flowing in and out. The remainder corresponded to water driven by waves through the *hoa*. Tidal amplitude in the lagoon were 50% lower than in the ocean, and there was a 4h lag between lagoon tides and ocean tides.

Based on this dataset, we successfully created a very simple parametric model with three calibrated coefficients to estimate cross-rim currents using only offshore wave conditions (Wave height and mean period), and the difference between offshore and lagoon water level. The model agrees well with the observations with RMSEs below 10% on all legs, for daily (detided) or hourly values. The model was able to simulate the currents with very good timing and good magnitude.

Moreover, the cross-rim currents model we implemented for semi-open Tuamotu atoll like Raroia relies on very few variables, that are available in plethora of water circulation models (e.g. water level inside or outside the lagoon) or through other readily available sources (offshore wave conditions from regional or global wave models). Therefore, it is now possible, if the three coefficients are known, to correctly and generically parameterize the flow through atoll rim *hoa*, as one of the boundary component of 3D lagoon models. Future work should include testing this parameterized model in other atoll settings and exploring if the values of the three model coefficients are generalizable. This is a significant step towards the development and use of numerical models for pearl farming management in Tuamotu atolls.

Authorship contribution statement

Jérôme Aucan : Conceptualization, Methodology, Formal analysis, Writing original draft

Romain Le Gendre : Conceptualization, Data curation, Writing, review and editing.

Terence Desclaux : Methodology, Formal analysis, Writing, review and editing.

Vetea Liao : Conceptualization, Funding acquisition, Writing, review and editing.

Serge Andréfouët : Conceptualization, Resources, Writing, review and editing, Supervision, Project administration, Funding acquisition.

Acknowledgements

This study was funded by the ANR-16-CE32-0004 MANA (Management of Atolls) project. Two oceanographic cruises MALIS 1 and MALIS 2, on board R/V Alis (https://doi.org/10.17600/18000582), also made this work possible. We are grateful to the R/V Alis crew, as well as to IRD, Ifremer and DRM electronicians and scientific divers: David Varillon, Bertrand Bourgeois, John Butscher, Chloe Germain, Joseph Campanozzi-Tarahu and Fabien Tertre. The study was co-funded by the DRM OTI project, Contrat de Projet France-French Polynesia, Program 123, Action 2, 2015–2020. Facilities at Tahiti were offered by IFREMER/CIP. We thank the 2 reviewers for their useful comments that helped improve the manuscript. We are also extremely grateful to Raroia's inhabitants and their Mayor for their help during fieldwork.

References

Andréfouët, S., Ardhuin, F., Queffeulou, P., Le Gendre, R., 2012. Island shadow effects and the wave climate of the Western Tuamotu Archipelago (French Polynesia) inferred from altimetry and numerical model data. Marine Pollution Bulletin 65, 415–424. URL: http://linkinghub.elsevier.com/retrieve/pii/S0025326X12002962, doi:10.1016/j.marpolbul.2012.05.042.

Andréfouët, S., Claereboudt, M., Matsakis, P., Pagès, J., Dufour, P., 2001a. Typology of atoll rims in Tuamotu Archipelago (French Polynesia) at landscape scale using SPOT HRV images. International Journal of Remote Sensing 22, 987–1004. doi:10.1080/014311601300074522.

Andréfouët, S., Genthon, P., Pelletier, B., Gendre, R.L., Friot, C., Smith, R., Liao, V., 2020. The lagoon geomorphology of pearl farming atolls in the Central Pacific Ocean revisited using detailed bathymetry data. Marine Pollution Bulletin 160, 111580. URL: http://www.sciencedirect.com/science/article/pii/S0025326X20306986, doi:https://doi.org/10.1016/j.marpolbul.2020.111580.

Andréfouët, S., Ouillon, S., Brinkman, R., Falter, J., Douillet, P., Wolk, F., Smith, R., Garen, P., Martinez, E., Laurent, V., Lo, C., Remoissenet, G., Scourzic, B., Gilbert, A., Deleersnijder, E., Steinberg, C., Choukroun, S., Buestel, D., 2006. Review of solutions

for 3D hydrodynamic modeling applied to aquaculture in South Pacific atoll lagoons. Marine Pollution Bulletin 52, 1138–1155. URL: http://linkinghub.elsevier.com/retrieve/pii/S0025326X06002852, doi:10.1016/j.marpolbul.2006.07.014.

Andréfouët, S., Pagès, J., Tartinville, B., 2001b. Water renewal time for classification of atoll lagoons in the Tuamotu Archipelago (French Polynesia). Coral Reefs 20, 399–408. URL: http://link.springer.com/10.1007/s00338-001-0190-9, doi:10.1007/s00338-001-0190-9.

Bessero, 1985. Marées. SHOM.

Bonneton, P., Lefebvre, J.P., Bretel, P., Ouillon, S., Douillet, P., 2007. Tidal modulation of wave-setup and wave-induced currents on the Aboré coral reef. Journal of Coastal Research Special Issue 50, 762 – 766 ICS2007. URL: https://hal.archives-ouvertes.fr/hal-00765727.

Caldwell, P.C., Aucan, J.P., 2007. An Empirical Method for Estimating Surf Heights from Deepwater Significant Wave Heights and Peak Periods in Coastal Zones with Narrow Shelves, Steep Bottom Slopes, and High Refraction. Journal of Coastal Research 23, 1237–1244. URL: https://doi.org/10.2112/04-0397R.1, doi:10.2112/04-0397R.1.

Callaghan, D.P., Nielsen, P., Cartwright, N., Gourlay, M.R., Baldock, T.E., 2006. Atoll lagoon flushing forced by waves. Coastal Engineering 53, 691–704. doi:10.1016/j.coastaleng.2006.02.006.

Charpy, L., Rodier, M., Fournier, J., Langlade, M.J., Gaertner-Mazouni, N., 2012. Physical and chemical control of the phytoplankton of Ahe lagoon, French Polynesia. Marine Pollution Bulletin 65, 471–477. URL: https://linkinghub.elsevier.com/retrieve/pii/S0025326X11006643, doi:10.1016/j.marpolbul.2011.12.026.

Chevalier, C., Sous, D., Devenon, J.L., Pagano, M., Rougier, G., Blanchot, J., 2015. Impact of cross-reef water fluxes on lagoon dynamics : a simple parameterization for coral lagoon circulation model, with application to the Ouano Lagoon, New Caledonia. Ocean Dynamics 65, 1509–1534. doi:10.1007/s10236-015-0879-x.

Codiga, D., 2011. Unified Tidal Analysis and Prediction Using the UTide Matlab Functions. Technical Report 2011-01. Graduate School of Oceanography, University of Rhode Island. Narragansett. URL: http://www.po.gso.uri.edu/ codiga/utide/utide.htm.

Dufour, P., Andrefouet, S., Charpy, L., Garcia, N., 2001. Atoll morphometry controls lagoon nutrient regime. Limnology and Oceanography 46, 456–461.

Dumas, F., Le Gendre, R., Thomas, Y., Andréfouët, S., 2012. Tidal flushing and wind driven circulation of Ahe atoll lagoon (Tuamotu Archipelago, French Polynesia) from in situ observations and numerical modelling. Marine Pollution Bulletin 65, 425–440. URL: https://linkinghub.elsevier.com/retrieve/pii/S0025326X12002950, doi:10.1016/j.marpolbul.2012.05.041.

Dutheil, C., Jullien, S., Aucan, J., Menkes, C., Le Gendre, R., Andréfouët, S., 2020. The wave regimes of the Central Pacific Ocean with a focus on pearl farming atolls. Marine Pollution Bulletin , 111751URL: http://www.sciencedirect.com/science/article/pii/S0025326X20308699, doi:10.1016/j.marpolbul.2020.111751.

Gourlay, M.R., Colleter, G., 2005. Wave-generated flow on coral reefs—an analysis for two-dimensional horizontal reef-tops with steep faces. Coastal Engineering 52, 353–387. URL: https://www.sciencedirect.com/science/article/pii/S037838390400170X, doi:https://doi.org/10.1016/j.coastaleng.2004.11.007.

Hearn, C.J., 1999. Wave-breaking hydrodynamics within coral reef systems and the effect of changing relative sea level. Journal of Geophysical Research: Oceans 104, 30007–30019. URL: https://agupubs.onlinelibrary.wiley.com/doi/abs/10.1029/1999JC900262.

Hench, J.L., Leichter, J.J., Monismith, S.G., 2008. Episodic circulation and exchange in a wave-driven coral reef and lagoon system. Limnology and Oceanography 53, 2681–2694. URL: http://doi.wiley.com/10.4319/lo.2008.53.6.2681, doi:10.4319/lo.2008.53.6.2681.

Kench, P.S., McLean, R.F., 2004. Hydrodynamics and sediment flux of hoa in an Indian Ocean atoll. Earth Surface Processes and Landforms 29, 933–953.

Lenhardt, X., 1991. Hydrodynamique des lagons d'atolls et d'ile haute en Polynésie Française. Ph.D. thesis. Mus. Nat. Histoire Nat.. Paris.

Lindhart, M., Rogers, J.S., Maticka, S.A., Woodson, C.B., Monismith, S.G., 2021. Wave modulation of flows on open and closed reefs. Journal of Geophysical Research: Oceans 126, e2020JC016645. doi:https://doi.org/10.1029/2020JC016645.

Lowe, R.J., Falter, J.L., 2015. Oceanic forcing of coral reefs. Annual Review of Marine Science 7, 43–66. doi:10.1146/annurev-marine-010814-015834.

Lowe, R.J., Falter, J.L., Monismith, S.G., Atkinson, M.J., 2009. Wave-Driven Circulation of a Coastal Reef-Lagoon System. Journal of Physical Oceanography 39. URL: http://journals.ametsoc.org/doi/abs/10.1175/2008JPO3958.1.

Merrifield, M.A., Becker, J.M., Ford, M., Yao, Y., 2014. Observations and estimates of wave-driven water level extremes at the marshall islands. Geophysical Research Letters 41, 7245–7253. doi:10.1002/2014GL061005.

Monismith, S.G., 2007. Hydrodynamics of Coral Reefs. Annu. Rev. Fluid Mech. 39, 37–55. doi:10.1146/annurev.fluid.38.050304.092125.

Monismith, S.G., Herdman, L.M.M., Ahmerkamp, S., Hench, J.L., 2013. Wave Transformation and Wave-Driven Flow across a Steep Coral Reef. Journal of Physical Oceanography 43, 1356 – 1379. URL: https://journals.ametsoc.org/view/journals/phoc/43/7/jpo-d-12-0164.1.xml, doi:10.1175/JPO-D-12-0164.1. place: Boston MA, USA Publisher: American Meteorological Society.

Pagès, J., Andréfouët, S., 2001. A reconnaissance approach for hydrology of atoll lagoons. Coral Reefs 20, 409–414. URL: http://link.springer.com/10.1007/s00338-001-0192-7, doi:10.1007/s00338-001-0192-7.

Rogers, J.S., Monismith, S.G., Fringer, O.B., Koweek, D.A., Dunbar, R.B., 2017. A coupled wave-hydrodynamic model of an atoll with high friction: Mechanisms for flow, connectivity, and ecological implications. Ocean Modelling 110, 66–82. URL: https://www.sciencedirect.com/science/article/pii/S146350031630169X, doi:https://doi.org/10.1016/j.ocemod.2016.12.012.

Sangare, N., Lo-Yat, A., Moullac, G.L., Pecquerie, L., Thomas, Y., Lefebvre, S., Gendre, R.L., Beliaeff, B., Andréfouët, S., 2020. Impact of environmental variability on Pinctada margaritifera life-history traits: A full life cycle deb modeling approach. Ecological Modelling 423, 109006. URL: http://www.sciencedirect.com/science/article/pii/S0304380020300788, doi:https://doi.org/10.1016/j.ecolmodel.2020.109006.

Symonds, G., Black, K.P., Young, I.R., 1995. Wave-driven flow over shallow reefs. Journal of Geophysical Research: Oceans 100, 2639–2648. doi:10.1029/94JC02736.

Tartinville, B., Rancher, J., 2000. Wave-induced flow over Mururoa atoll reef. Journal of Coastal Research , 776–781.

Table 1: Site instrumentation and positions

Site	Latitude (S)	longitude (W)	variable measured	Make and model	Sampling rate
H1	15.997	142.433	current and water level	Nortek Aquadopp	5 min bursts
H2	16.035	142.346	current and water level	Nortek Aquadopp	5 min bursts
H3	16.241	142.479	current and water level	Nortek Aquadopp	5 min bursts
H5	16.115	142.382	current and water level	Nortek Aquadopp	5 min bursts
L4	15.987	142.364	wave and water level	RBR Duet	continuous 1 second
L5	16.065	142.419	wave and water level	RBR Duet	continuous 1 second
L6	16.151	142.469	wave and water level	RBR Duet	continuous 1 second
L7	16.118	142.503	wave and water level	RBR Duet	continuous 1 second
L8	16.153	142.411	wave and water level	RBR Duet	continuous 1 second
O1	15.994	142.437	wave and water level	RBR Duet	continuous 1 second
O2	16.037	142.341	wave and water level	RBR Duet	continuous 1 second
O3	16.249	142.480	wave and water level	RBR Duet	continuous 1 second

Table 2: Total hourly sea level variance explained by the tidal analysis (in %) and tidal harmonics amplitude (cm) for the principal semidiurnal (M2, N2, S2 and K2) and diurnal (K1) tidal constituents at the different sites

	Ocean sites			Lagoon sites				
	O1	O2	O3	L4	L5	L6	L7	L8
Variance explained	98.3	98.3	97.9	70.5	70.3	70.9	70.3	70.5
M2	32.3	33.1	29.8	15.8	15.8	15.9	15.9	15.9
N2	7.1	7.5	6.7	3.3	3.3	3.3	3.3	3.3
S2	6.1	6.6	6.7	2.1	2.1	2.1	2.1	2.1
K1	2.5	1.8	2.1	1.7	1.7	1.8	1.7	1.8
K2	2.1	2.3	2.4	0.9	0.9	1.0	1.0	0.9

Table 3: Tidal phase lag (h) for the principal semidiurnal (M2, N2, S2 and K2) and diurnal (K1) tidal constituents at the different sites relative to tidal phase at O1

	Ocean sites			Lagoon sites				
	O1	O2	O3	L4	L5	L6	L7	L8
M2	0.0	-0.3	-0.4	4.4	4.4	4.4	4.4	4.4
N2	0.0	-0.4	-0.3	4.5	4.5	4.5	4.5	4.5
S2	0.0	-0.4	-0.4	6.2	6.2	6.1	6.1	6.2
K1	0.0	0.3	-0.0	3.6	3.6	3.7	3.6	3.6
K2	0.0	-0.2	-0.1	4.9	4.9	4.9	4.9	4.9

Table 4: A and C parameter values in equation 1 calculated for each leg , correlation and range-normalized RMSE (%) between modeled and daily-averaged observations.

	A	C	Correlation	RMSE(%)
H1 Leg3	0.178	-0.179	0.976	5.1
H2 Leg1	0.125	-0.195	0.987	3.6
H2 Leg2	0.110	-0.157	0.986	3.5
H2 Leg3	0.082	-0.079	0.857	9.7
H3 Leg1	0.099	-0.175	0.966	5.1
H3 Leg2	0.083	-0.124	0.959	6.7
Mean	0.113	-0.151		

Table 5: Correlation (r) and range-normalized RMSE (%) between modeled and daily-averaged observations when using equation 1 and mean values of A and C parameters, cf Table 4.

	Correlation	RMSE(%)
H1 Leg3	0.975	32.1
H2 Leg1	0.986	4.4
H2 Leg2	0.986	5.0
H2 Leg3	0.857	11.5
H3 Leg1	0.966	16.1
H3 Leg2	0.959	24.2

Table 6: A, B, and C parameter values in equation 2 calculated for each leg , correlation and range-normalized RMSE (%) between model and hourly observation.

	A	B	C	Correlation	RMSE(%)
H1 Leg3	0.191	0.584	-0.213	0.971	4.2
H2 Leg1	0.172	0.551	-0.343	0.911	8.1
H2 Leg2	0.148	0.450	-0.270	0.900	8.5
H2 Leg3	0.096	0.397	-0.114	0.832	8.8
H3 Leg1	0.115	0.291	-0.224	0.935	6.1
H3 Leg2	0.103	0.285	-0.183	0.916	7.9
Mean	0.138	0.427	-0.225		

Table 7: Correlation (r) and range-normalized RMSE (%) between model and observation when using equation 2 and mean values of A, B and C parameters, cf Table 6 .

	Correlation	RMSE(%)
H1 Leg3	0.971	16.5
H2 Leg1	0.911	9.1
H2 Leg2	0.900	8.7
H2 Leg3	0.825	9.3
H3 Leg1	0.929	11.9
H3 Leg2	0.914	15.9

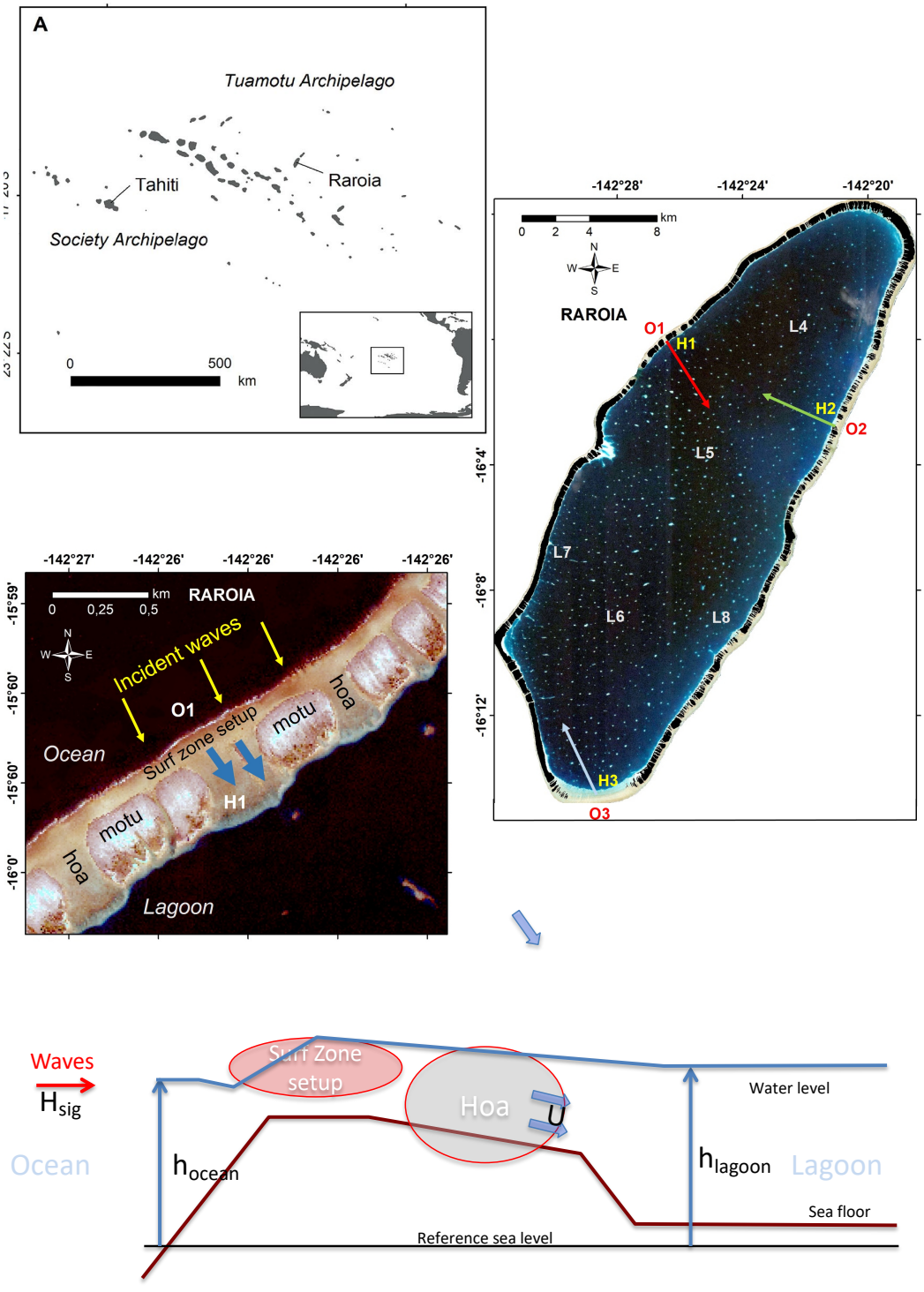

Figure 1: Top : Location map of the Raroia atoll, niddle right, with location of the instruments. Arrows indicate principal direction of current discussed in section 2.2. middle left : Typical instrument configuration near site 1. Bottom : Schematics of site along with observed variables.

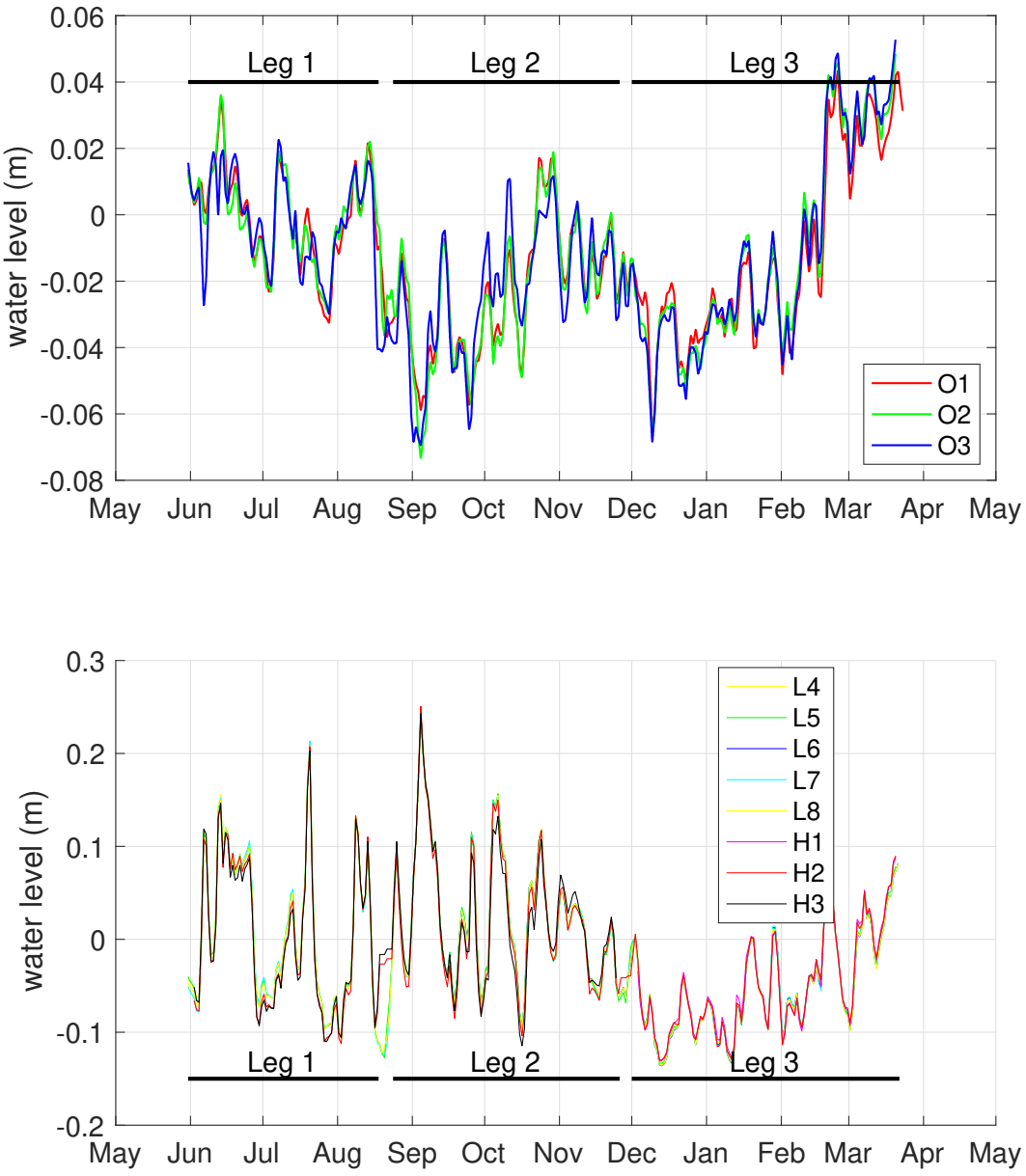

Figure 2: Water level at the 3 ocean sites (top) and at the 5 lagoon and 3 *hoa* sites (bottom). Water levels are shown relative to the time-average water level at each station. Leg durations are indicated in black.

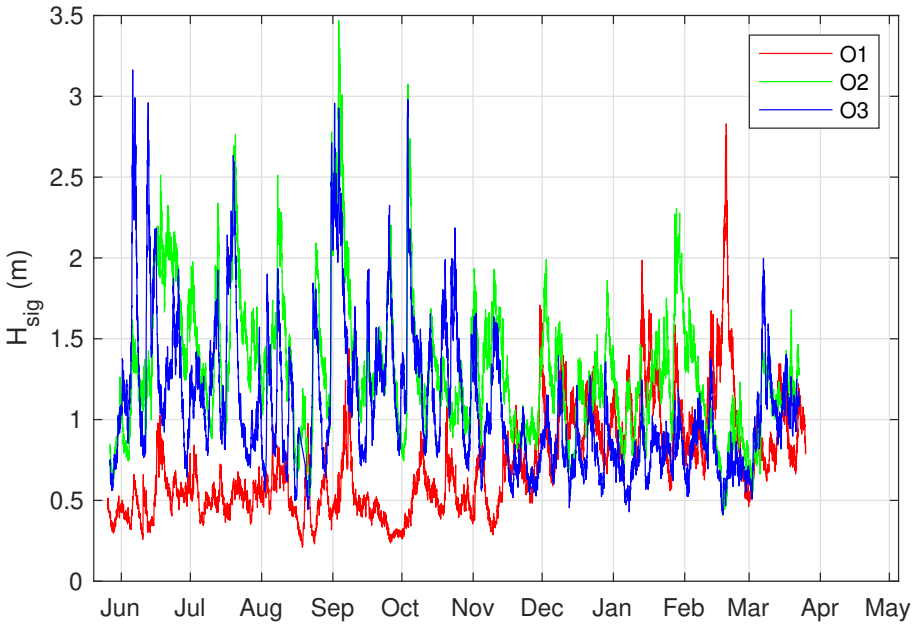

Figure 3: Wave height at the ocean sites O1 (red), O2 (green) and O3 (blue)

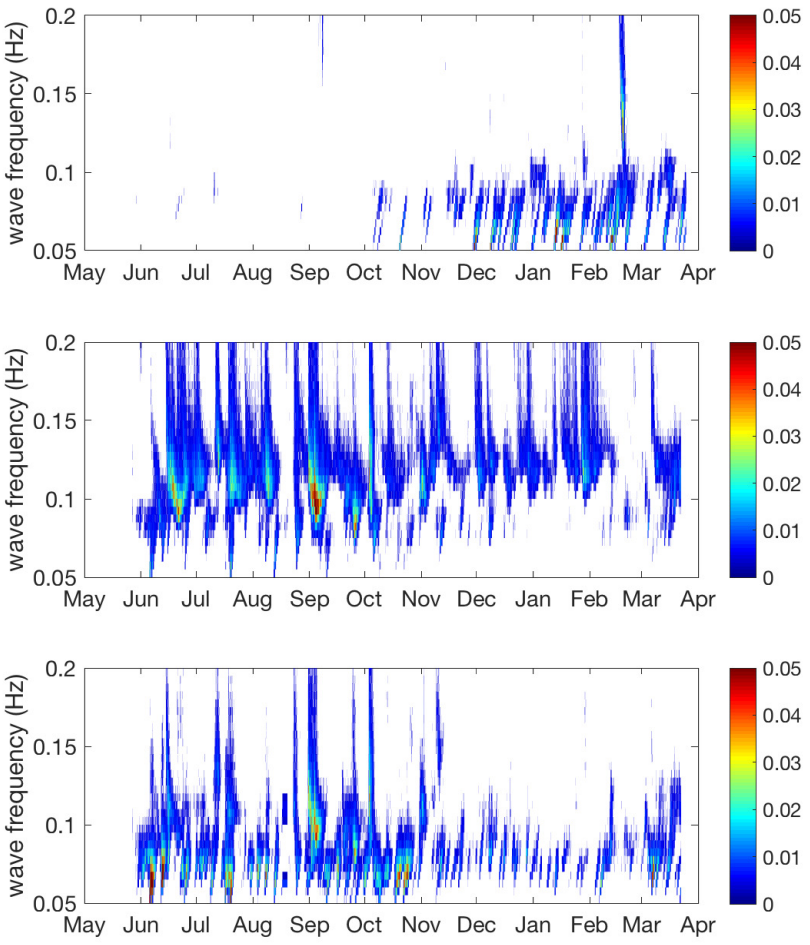

Figure 4: Water level spectrogram ($S(f)$, in m^2) at the ocean sites O1 (top), O2 (middle) and O3 (bottom).

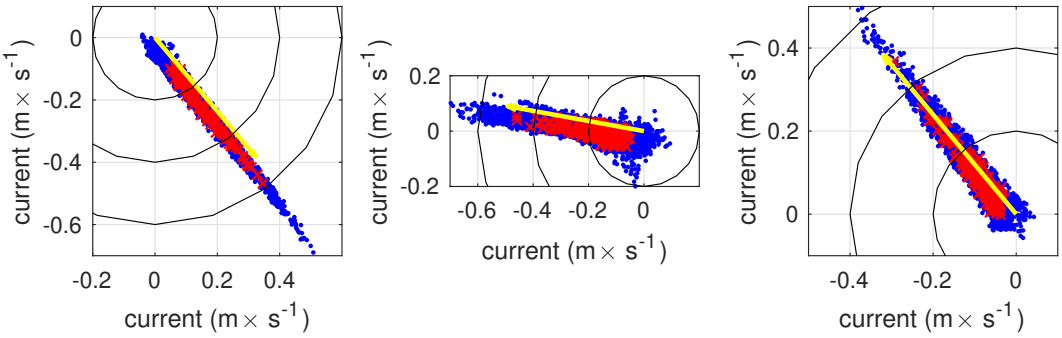

Figure 5: Hourly (blue) and daily (red) averaged E-N current vectors at site H1 (left), H2 (center) and H3 (right). Principal directions are indicated in yellow.

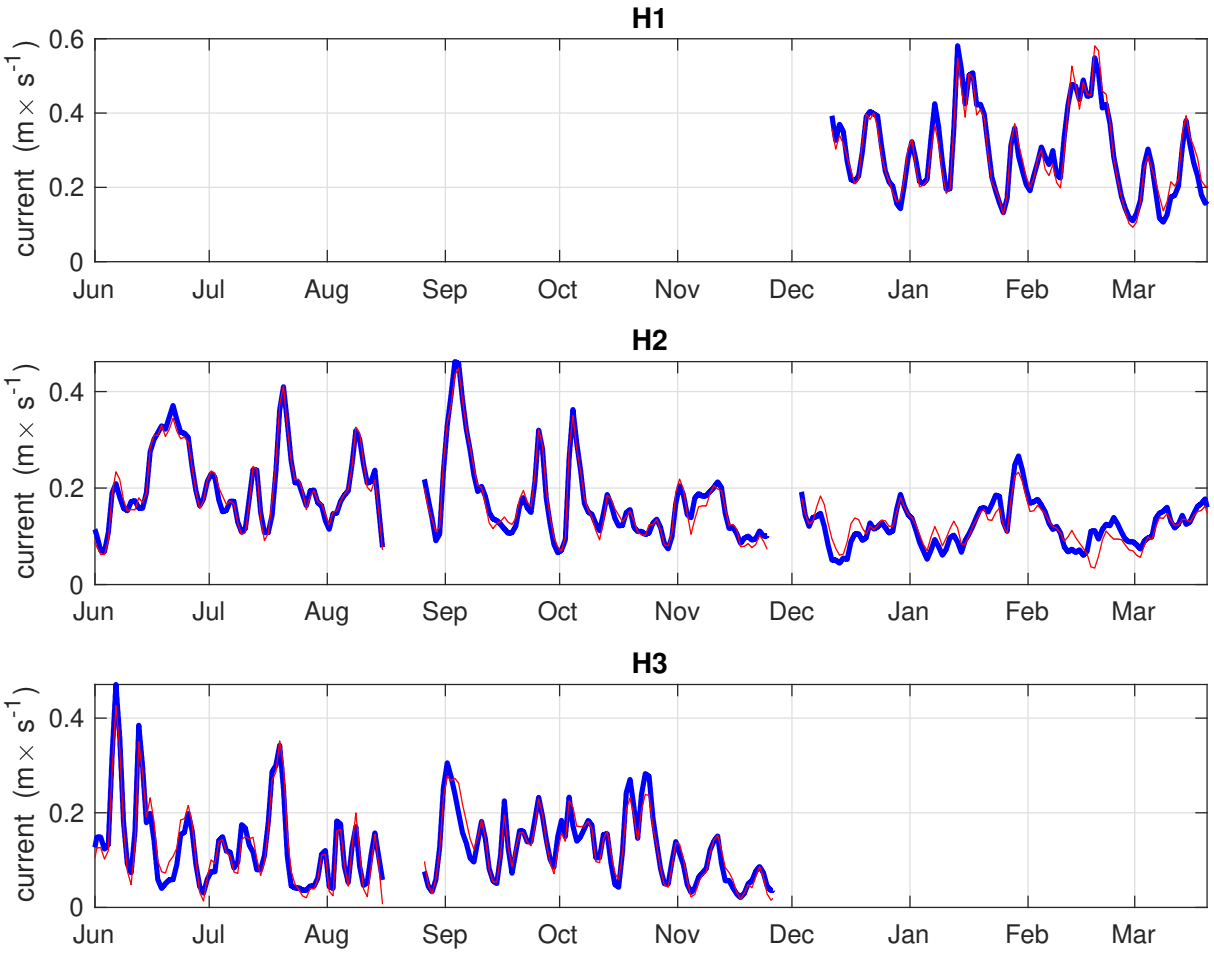

Figure 6: Daily average current speed in the hoa at the different legs and sites, measured (thick blue line), and modeled (thin red line) using equation 1 .

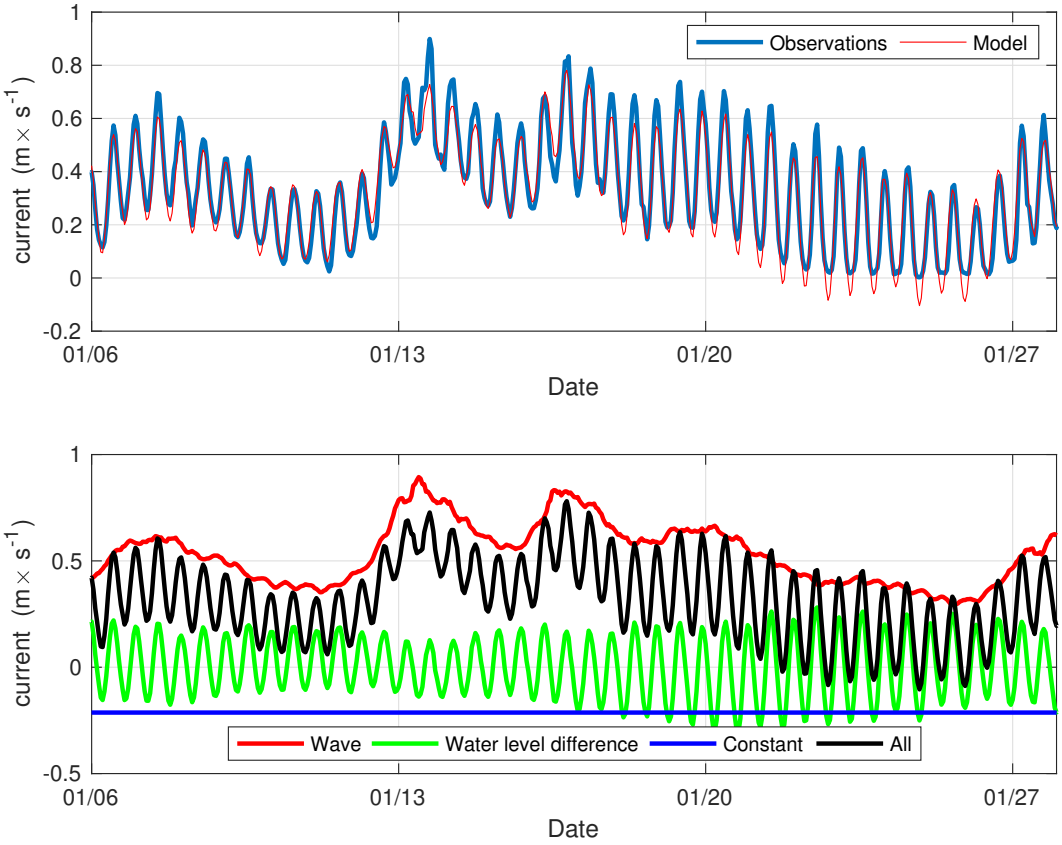

Figure 7: Example of hourly averaged speed in the hoa at H1 during leg 3, measured (thick blue line), and modeled (dashed red line) using equation 2. Example of individual contributions of terms in equation 2 .